Journal of Materials Chemistry C

Accepted Manuscript

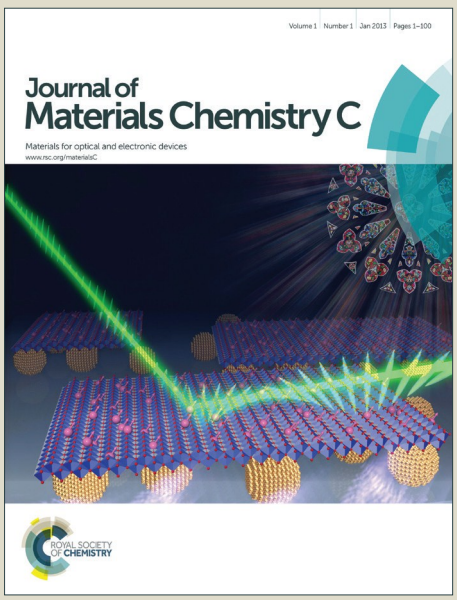

ROYAL SOCIETY OF CHEMISTRY

www.rsc.org/materialsC

Journal of

Materials Chemistry C

ARTICLE

Fabrication of 2D and 3D photonic crystal arrays towards metal ions or biomolecule high performance recognition

Received 00th January 20xx,
Accepted 00th January 20xx

DOI: 10.1039/x0xx00000x

www.rsc.org/

Ting Chen, [b] Zheng-Yan Deng, [b] Su-Na Yin, [b] Su Chen*[b] and Chen Xu*[a]

Methods allowing photonic crystals to be carried out on metal-ion recognition and biological detection in a controllable fashion are potentially important for analytic chemistry. Herein, 2D photonic crystal films and 3D photonic crystal supraballs were respectively prepared to serve as the inkjet printing response and single loaded coordination response, detecting metal ions. Subsequently, we describe a cell photonic crystal array (CPA) chip, coupling functionalized 3D photonic crystal supraballs with 96-well plate, establishing a testing platform. By using microplate reader, multiple signals could be extracted at once, which simplifies the testing process and saves the detection time. This simple and convenient method is expected to be applied to qualitative and quantitative tests of various heavy metal ions and biomolecules, such as BSA, a kind of biological macromolecules.

Introduction

Photonic crystals (PCs), possessing extraordinary optical properties, bright structural color and characteristic photonic band-gaps, have been widely employed in numerous fields, such as optical devices,[1-8] catalytic reaction,[9-14] detection,[15-25] and various sensors[26-41]. Especially, photonic crystal sensors for heavy metal ions,[42-44] biomolecules,[45-50] relevant materials[51-54] in the fields of biological and chemical detection have been broadly reported and provide a low-cost and feasible approach to distinguish diverse external stimuli. Furthermore, to analyze high-throughput sensing data, sensor array technologies[55-64] have been increasingly applied for detection, especially on converting single to multiple detection signals via visible process. In this perspective, Cunningham et al.[65-66] extended the detection capabilities of a standard microarray test with a photonic crystal surface to enhance observing fluorescence from microarray spots, making it possible to reliable trace detection of DNA with standard substrates poss by increasing the dynamic range of surface-bound fluorescence-based assay. Song et al.[67] provided a multi-stopband photonic crystal microchip fabricated based on a surface modified indium tin oxide (ITO) glass as patterned substrate, selectively strengthening the sensing fluorescence signal in various channels and proposing a more efficient multi-analyte discriminant detection. Li et al.[68] prepared molecularly imprinted inverse-opal photonic polymers (MIPPs) serving as sensing elements with desired features, such as the high sensitivity and selectivity, to construct sensor arrays by combining molecular imprinting and colloidal crystal template. Gu et al.[69] raised a fluorescent dye doped mesoporous colloidal crystals vapor sensing chip holding splendid selectivity and repeatability to discriminate various kinds of vapors of different concentrations, which could be potentially expanded to the detection of other gases and mixed gases. Although a wide variety of sensor arrays have been developed for identifying variant kinds of chemicals, disadvantages still exist, such as signal singularity, lack of corresponding platform, inconvenience of information extraction and incomplete system. Therefore, it is still a challenge to develop a facile method to construct a sensor array with miniaturization, integration and high sensitivity, especially applicable for the detection of biomolecules.

In this work, we demonstrate an available method for establishing 96-well plate based 3D photonic crystal (PC) supraballs platform, which enables it to analyze metal ions and biomolecules with high efficiency and simplicity of extracting information. Initially, these supraballs were constructed using monodispersed polystyrene colloids with the addition of 8-hydroxyquinoline (8-HQ), to serve as 3D PC microdetector towards metal ions. Subsequently, 2D PC films were fabricated via vertical deposition method to investigate the effects of different stop-bands on the fluorescence intensity of 8-HQ/Zn^{2+} complex via inkjet printing technology. Moreover, we applied these supraballs to construct fluorescent probe platform and a cell photonic crystal array (CPA) chip, allowing them to quantitative determination of bovine serum albumin (BSA) and 11 kinds of metal ions with 10^{-8} mM level. This approach provides a facile and effective method, allowing 96

[a] *State Key Laboratory of Pharmaceutical Biotechnology, School of Life Sciences, Nanjing University, 163 Xianlin Road, Nanjing 210023, P. R. China.*
E-mail: xuchn@nju.edu.cn
[b] *State Key Laboratory of Materials-Oriented Chemical Engineering, College of Chemistry and Chemical Engineering, Nanjing Tech University (the former: Nanjing University of Technology), No. 5 Xin Mofan Road, Nanjing 210009, P. R. China.*
E-mail: chensu@njtech.edu.cn

signals extraction at a time. This offers the possibility to build platform for facilely detecting various other analytes.

Experimental

Materials

Styrene (St) was purified by distillation under reduced vacuum to remove inhibitor. Potassium persulfate (KPS) was purified by recrystallization from water. 8-hydroxyquinoline (8-HQ), fluorescamine (FL), tetraethylenepentamine (5N) and sodium bicarbonate ($NaHCO_3$) were purchased from Sinopharm Chemical Reagent Co., Ltd. $AlCl_3$, $ZnCl_2$, $CdCl_2$, $MgCl_2$, LiCl, $PbCl_2$, $MnCl_2$, $CoCl_2$, $NiCl_2$, $CuCl_2$ and $FeCl_3$ were supplied by Shanghai Ling Feng Chemical Co., Ltd., and used as purchased without further purification. Bovine serum albumin (BSA) was purchased from Shanghai Hui Xing biochemical reagent Co., Ltd. High-purity water (resistivity, ~18 $M\Omega.cm^{-1}$) was used throughout these experiments. Polyvinylpyrrolidone (PVP), absolute ethanol (99.5 %) were of analytical grade, commercially available and used without any further purification.

Synthesis of Monodispersed polystyrene (PS) colloidal particles

Monodispersed polystyrene particles were prepared by emulsion polymerization. 1.0 g $NaHCO_3$ and 0.3 g PVP were added into a 250 mL round bottom flask with four necks, with 135 mL deionized water as solvent. After 30 min sufficiently stirring under a nitrogen atmosphere, 7.5 g monomer was dropped in. As the temperature of solution rising quickly to 98 ^{o}C, 0.04 g KPS dissolved in water was dripped slowly into the flask. The polymerization was carried out at constant condition for 3 h.

Preparation of 2D PC films

Prior to the film forming process: to obtain hydrophilic substrates, glass slides were treated by piranha solution containing 96 % H_2SO_4, 33 % H_2O_2 and water (H_2SO_4:H_2O_2:H_2O = 6:3:2 v/v/v. Warning! Piranha solution is considerably dangerous as strong acid and oxidizer, which can explode!) for 24 h. Then, the substrates were washed with purified water several times and dried in nitrogen condition for use. Photonic crystal films were fabricated by vertical deposition method. The substrates were inserted into prepared monodispersed polystyrene dispersion of which the concentration was 0.2 wt%. The beakers were placed in constant temperature humidity chamber for 18 h with the temperature keeping at 60 ^{o}C and the humidity maintaining at 80 %. Along with the evaporation of solvent, colloid particles collected in the substrate-air-liquid interface self-assembled to form single layer or multi-layer colloid photonic crystal.

Patterning from Zn^{2+}/H_2O into the 2D PC films

1.0 mM 8-HQ and polyvinylpyrrolidone (0.5 % PVP in anhydrous ethanol) solution was firstly pipetted onto each PC film. Then the solution was filled in the interspaces of the colloidal particles with the action of capillary force. After the solvent evaporated, the 8-HQ solution was functionalized onto the PC films. For inkjet printing, 5 g Zn^{2+} solution (1.0 mM in water, pH = 5) was encapsulated into the ink cartridge of Dimatix DMP 2831 inkjet printer for printing at room temperature. The printing process was realized in 20 min.

Preparation of 3D PC supraballs.

A simple microfluidic device was applied to produce 3D PC supraballs, which used the aqueous solution of monodispersed polystyrene (PS) microspheres as the discontinuous phase in one needle and the methylsilicone oil in the PDMS capillary as the continuous phase, respectively. The flows of PS solution was broken by the continuous phase of methylsilicone oil at the tip of needles, flowing along the capillary tube into a polyethylene container, which were then heated at 45 ^{o}C for 12 h to allow water evaporation. Subsequently, the supraballs were thoroughly washed with hexane to remove the methyl superficial silicone oil on the surface.

Characterization

The morphology of the 2D PC films and 3D PC supraballs were observed by scanning electron microscopy (SEM) with a QUANTA 200 (Philips-FEI, Holland) instrument at 20.0 kV. The films and supraballs were also observed by an inverted fluorescence microscope (SFM-30I, Shanghai). Photographic images of the samples were captured by digital camera (100IS, Canon) or stereomicroscope (SZM45). Photoluminescence (PL) spectra were measured on a Varian Cary Eclipse spectrophotometer at room temperature. A 420 nm laser beam was chosen as the excited light source from a Xe lamp with the voltage of 700 V, and the excitation and emission slits were both 5 nm. The fluorescence images were taken using an Olympus MVX10 stereomicroscope with color CCD camera. Reflection spectra were recorded by a UV-vis spectrometer (Lambda 950, Perkin-Elmer) in reflection mode. Angle-dependent measurements of photoluminescence (PL) spectra were carried out using a Varian Cary Eclipse spectrofluorometer with a 450 nm laser beam as a light source. For time-resolved fluorescence spectra (SLM 48000DSCF spectrofluorometer), we used a pulsed He laser, which emits at 405 nm and has a pulse width of 100 ps. The spontaneously emitted light was detected from the surface facing away from the excitation beam at an angler relative to the (111) planes. Fluorescence measurements were performed with microplate reader (Tecan Safire, Crailsheim, Germany) and IVIS Lumina XR imaging system (Caliper Instruments, Alameda, CA, USA).

Results and discussion

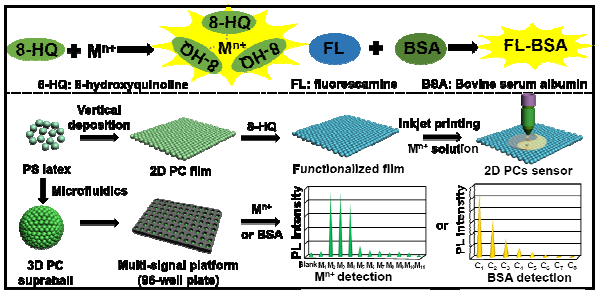

Scheme 1. Schematic representation of testing basis of metal ions and BSA, functionalized 2D PC film towards analysis of zinc ions or 3D PC supraballs arrays towards analysis of metal ions and BSA analytes.

Scheme 1 represents testing basis of metal ions and BSA: functionalized 2D PC film towards analysis of zinc ions or 3D PC supraballs arrays towards analysis of metal ions and BSA analytes. As displayed in Scheme 1, we fabricated 2D PC films using monodispersed PS colloidal via vertical deposition method and modified them with 8-HQ. After inkjet printing zinc ions, a pattern containing PL signal of zinc ions was formed. Also, we constructed 3D PC supraballs by microfluidic technology and arranged them to 96-well plate, establishing 96-well plate based 3D PC supraballs platform, which enables it to analyze 11 kinds of metal ions and BSA according to their varieties of fluorescent intensity.

Preparation of fluorescent-marking 2D photonic crystal films toward Inkjet sensing Zn^{2+} ion.

Typically, 8-hydroxyquinoline (8-HQ), possessing capability for coordinating with different kinds of metal ions, is applied to analyze different kinds of metal ions. However, its fluorescence signal is too weak to identify the analytes. In this case, after coupling 8-HQ with the PS PCs, the detection sensitivity can be enhanced 20-100 times by aid of overlapping two kinds of signals, 8-HQ/M^{n+} fluorescent and PS PC stop-band signals. Herein, 8-HQ and FL-5N, for instance, were adopted to realize metal-ion recognition or concentration measurement of BSA.

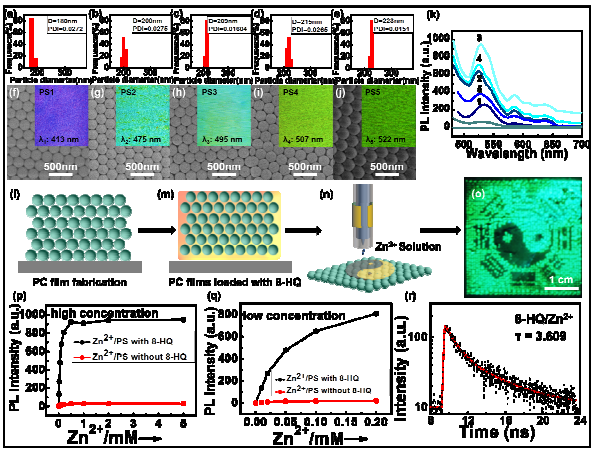

Figure 1. (a-e) DLS (Dynamic light scattering) data of monodispersed polystyrene colloidal particles; (f-j) SEM top-view images of PC films (Insert: Metallographic microscope photographs of prepared colloidal photonic crystal films (The reflection spectrum of each PC film shown on the bottom of each photograph)); (k) The 8-HQ/Zn^{2+} (1 mM) response fluorescence spectra on PS films with different stopbands; (l-n) Perspective view to fabricate functionalized colloidal photonic crystal films and piezoelectric inkjet printing process; (o) Photographs of fluorescent "Tai Chi" pattern by piezoelectric inkjet printing on the 3th PC film under UV light. Scale bar: 1 cm; (p) The Zn^{2+} concentration dependence of the fluorescence at 530 nm on PS3 and on a blank surface; (q) Detail of the low concentration (0-200 μM) region; (r) A typical time-resolved fluorescence decay curve of 8-HQ/Zn^{2+} (λ_{ex} = 405 nm) measured at the fluorescence peak of 530 nm.

Figure 1a-e show the DLS (Dynamic light scattering) data of monodispersed polystyrene colloidal particles, corresponding five different diameters of 180 nm (PS1), 200 nm (PS2), 209 nm (PS3), 215 nm (PS4), 223 nm (PS5), used to fabricate 2D PC films. And the stopbands noticed at 413 nm (PS1), 475 nm (PS2), 495 nm (PS3), 507 nm (PS4) and 522 nm (PS5), are corresponding to PS particle sizes above, respectively. Whereas the iridescent structure colors of PC films are violet, blue, light blue, green and dark green as exhibited inserted in each SEM image (Figure 1f-j). These scanning electron microscope (SEM) images show that the colloidal particles are in a face-centered cubic arrangement with a close-packed plane (111) oriented parallel to the substrate. To investigate the relationship between the stopband of PC and fluorescence spectra of metalloquinoline, we applied the PC films as the template substrates and Zn^{2+}/H_2O solution as ink for inkjet printing. Figure 1l-n obviously shows the processing to functionalize the as-prepared PC films with 8-HQ and piezoelectric inkjet printing of Zn^{2+}/H_2O solution into substrate. Subsequently, 1.0 mM 8-HQ and polyvinylpyrrolidone (0.5 % PVP in anhydrous ethanol) solution was firstly pipetted onto each PC film. Then, the solution filled into the interspaces of the colloidal particles with the action of capillary force. After the solvent evaporated, the 8-HQ sensor

molecules were dispersed in PVP and filled in the interspaces of the PC matrix. Therefore, the 8-HQ sensor was functionalized onto the PC films. Then, the prepared Zn^{2+}/H_2O solution was used as ink to inject on these PC films, respectively. Yellow-green fluorescent images with different intensities are formed on the functional PC film substrates in several seconds. The fluorescent intensities of the above five "Tai Chi" images are shown in Figure 1o. Apparently, the PS3 film displays a brighter yellow-green emission under UV light (365 nm) (Figure 1k), so the PS3 is chosen to be the appropriate photonic crystal to match the 525 nm fluorescence for later research. Moreover, the as-prepared 2D PC film herein contains optical structural color and 8-HQ/Zn^{2+} fluorescent dual signals, which have good sensitivity and can be expended to the analysis of other metal ions.

We further quantitatively analyze the fluorescent intensities of the "Tai Chi" images. A Zn^{2+} concentration-dependence investigation of the fluorescence on PS3 (PC film loaded with 8-HQ) and blank surface (PC film unloaded with 8-HQ) presents the apparent fluorescence enhancement and detection sensitivity improvement (Figure 1p-q). Moreover, the fluorescence lifetime (τ) of 8-HQ/Zn^{2+} was assessed by time-resolved photoluminescence (PL) measurements. As seen in Figure 1r, the decay trace for 8-HQ/Zn^{2+} is fitted using biexponential functions Y(t) based on non-linear least squares analysis in Equation (1).

$$Y(t) = \alpha_1 \exp(-t/\tau_1) + \alpha_2 \exp(-t/\tau_2)$$

Where α_1 and α_2 are fractional contributions of time-resolved decay lifetime τ_1, τ_2 and, average lifetime $\bar{\tau}$ could be concluded from the equal (2):

$$\bar{\tau} = \frac{\alpha_1\tau_1^2 + \alpha_2\tau_2^2}{\alpha_1\tau_1 + \alpha_2\tau_2}$$

We calculated the average lifetime $\bar{\tau}$ of 8-HQ/Zn^{2+} as 3.61 ± 0.05 ns, which was comparable to reported values. The reason for increased fluorescence-decay time is that PVP polymer contains coordinating groups with Zn^{2+} ions in this hybrid, and then avoids non-radiative recombination. The rink-amide groups with strong polarity and hydrogen bond in the molecular structure of PVP, as well as the atoms and nitrogen atoms to be typical coordination atoms, enable it to complex with several metals or some compounds containing hydroxyl, carboxyl, amino and other active hydrogen atoms. Besides, from the molecular structure of view, oxygen atom is bare, while the nitrogen atom is surrounded by methyl and methylene, so that it has a surface activity to show favourable adsorption to a solid surface and enable it to stay on the surface of PS colloidal particle.

Preparation of 3D PC supraballs via microfluidic and fluorescent-marking 3D PC supraballs toward construction of detecting metal ions platform.

Based on preliminary tests of metal ions with 2D PC films, 3D PC supraballs are produced to serve as the single loaded coordination response (SLCR). A typical microfluidic flow-focusing device is applied to prepare the 3D PC supraballs and the specific structure is illustrated in Figure 2a. The diameter of monodispersed polystyrene we used here is 209 nm. After assembly, brilliant colors appeared on the surface of supraballs following water evaporation from the spherical droplets (Figure 2b). The color of cyan is found and the reflected wavelength of correspondent PC supraball is at 525 nm, the specular reflectivity peak, the so-called stop-band, is apparently observed (Figure 2d). It is explicit that each supraball is within a given batch presenting outstanding uniformity in size and arranging into close-packed lattices (Figure 2c).

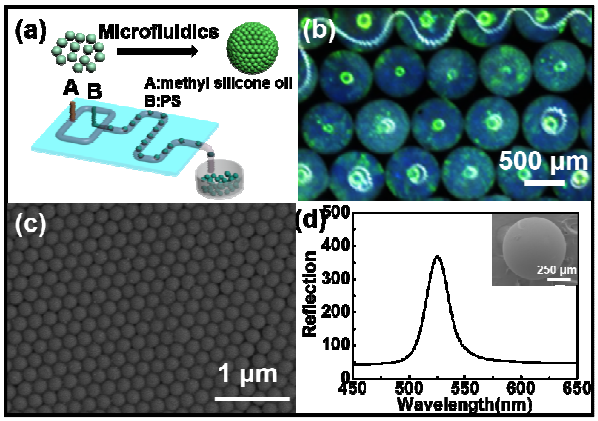

Figure 2. (a) Fabrication of 3D PC supraballs; (b) Optical microscope images of prepared PC supraballs. Scale bar: 500 μm; (c) Close-packed lattices on the surface of PC supraball; (d) Reflectance spectrum of prepared PC supraballs. Insert: SEM of a single PC supraball.

Besides 8-HQ, FL-5N loaded PC supraballs can also exhibit the analogous fluorescence enhancement and quenching effect when it is coordinated with diverse metal ions. The principles of metal complexes are expressed as illustrated in Figure 3a. Functional compounds, like 8-HQ and FL-5N, were pipetted into 3D PC supraballs, following the solvent drying. Al^{3+}, Zn^{2+}, Cd^{2+}, Li^{+}, Mg^{2+}, Pb^{2+}, Mn^{2+}, Co^{2+}, Ni^{2+}, Fe^{3+} and Cu^{2+} (1.0 mM in water, pH = 5) solutions were respectively pipetted into the as-prepared 3D PC supraballs. Figure 3b schematically illustrates the simple operation procedure.

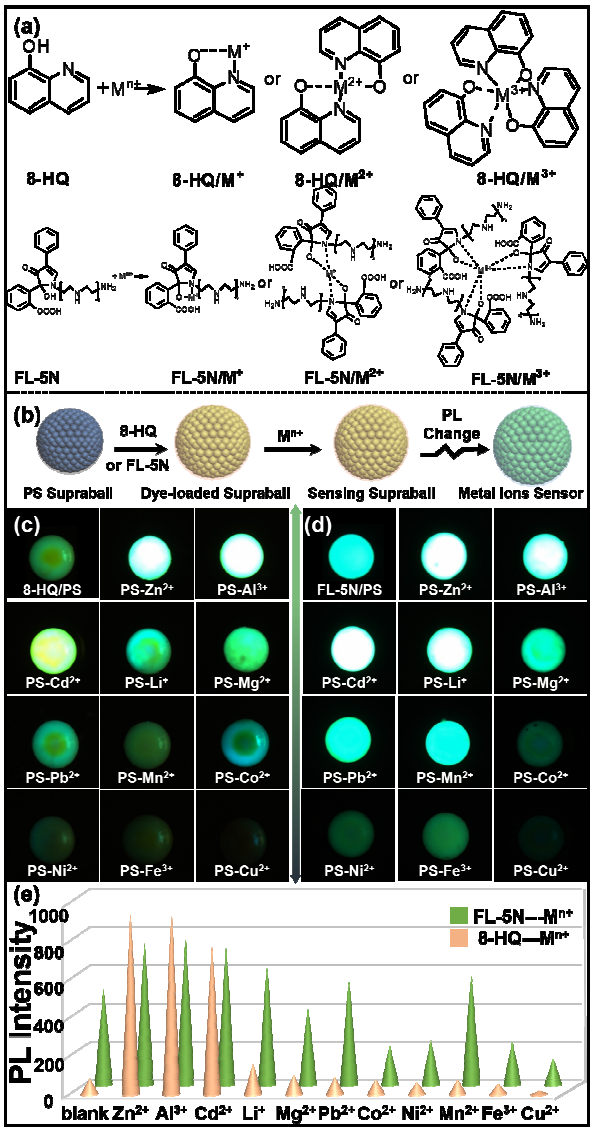

Figure 3. (a) Complexing principle of cation with 8-HQ and FL-5N; (b) Process to functionalize the PC supraballs with functional compounds 8-HQ and FL-5N; (c-d) Fluorescence images of 11 metal ions (1.0 mM in water, pH = 5) on prepared 8-HQ-PCs and FL-5N-PCs supraballs; (e) Patterns of 11 metal ions responses of 8-HQ-PCs and FL-5N-PCs supraballs.

The 3D PC supraballs containing functional compound and one polyvinylpyrrolidone (PVP) row as the control sample are provided for comparative study. 8-HQ and FL-5N are loaded onto the PC supraballs and PVP control samples. The fluorescence responses of the functionalized PC supraballs to the presence of 11 metal ions (Al^{3+}, Zn^{2+}, Cd^{2+}, Li^{+}, Mg^{2+}, Pb^{2+}, Mn^{2+}, Co^{2+}, Ni^{2+}, Fe^{3+} and Cu^{2+}) are recorded in 8-HQ and FL-5N functionalized PC supraballs. The fluorescent images are obtained when the PC supraballs are dried, which show obvious fluorescence shifts for each supraball (Figure 3c-d). The phenomenon in Figure 3c demonstrates the selective fluorescence enhancement and quenching because of the slow photon effect of PC. Transparently, Al^{3+}, Zn^{2+}, Cd^{2+} electron-transfer with sensor receptor contribute the fluorescence enhancement or red-shift, the fluorescent intensity of Li^{+}, Mg^{2+}, Pb^{2+}, Mn^{2+}doped samples are appreciably enhanced, while those of, Co^{2+}, Ni^{2+}, Fe^{3+}, Cu^{2+} samples are quenched. Based on photonic crystal structures, the group velocity of light decreases when approaching the band edge of the band-gap. At this point, photons couple with a local resonance mode and Bragg scatter out of the structure, which greatly enhances the interaction of light with matter. What is more, this high density of states near the stopband would enhance the coupling of spontaneously emitted photons to these modes.[18, 70, 71] Analogously, the fluorescence intensity of the metal ion on the FL-5N functionalized photonic crystal beads has a similar enhancement or quenching effect (Figure 3d). Obviously, the changes of fluorescence intensities match to the fluorescent images (Figure 3e). As a result, functional compounds combined with different metal ions will result in the enhancing/quenching or red-shift of the fluorescence spectra, furnishing possibility to construct microreactor for the detection of metal ions independently and macroscopically.

The platform construction of 96-well plate simultaneous fluorescence responses toward qualitatively analyzing metal ions.

In order to systematacially explore the fluorescence responses, we use 8-HQ doped 3D PC supraballs as single loaded coordination response (SLCR), combining them with a 96-well plate, to form the cell photonic crystal array (CPA) chip. 1.0 mM 8-HQ and polyvinylpyrrolidone (0.5 % PVP in anhydrous ethanol) solution was dropped into the holes of the 96-well plate using micropipette (50 μL), before which the holes were filled with PC supraballs. After the solvent evaporated, different concentration (10^{-3} - 10^{-8} mM) of 11 metal ions in solutions (50 μL) were added into the wells respectively. The fluorescence responses were detected by automatic microplate reader in five distinct channels (CH1: 530 nm with 430 nm excitation, CH2: 500 nm with 430 nm excitation, CH3: 470 nm with 390 nm excitation, CH4: 530 nm with 390 nm excitation, CH5: 500 nm with 390 nm excitation, represented by different colors as yellow, red, dark blue, green and light blue), exhibiting visibly distinct fluorescence intensities from each well.

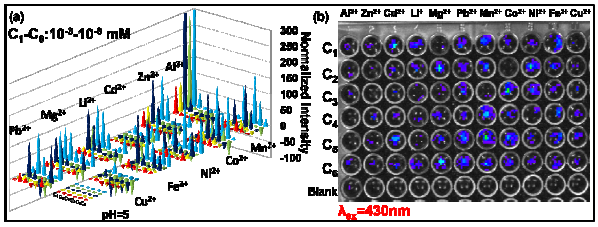

Figure 4. (a) Patterns of 11 metal ions (Al^{3+}, Zn^{2+}, Cd^{2+}, Li^{+}, Mg^{2+}, Pb^{2+}, Mn^{2+}, Co^{2+}, Ni^{2+}, Fe^{3+} and Cu^{2+}) of the concentration (10^{-3} - 10^{-8} mM) region responses of 8-HQ/M^{n+} PC array. The fluorescence change induced in five independent excitation and emission channels (Represented by different colors). The pyramids pointing down correspond to negative intensity values and indicate fluorescence quenching while the pyramids pointing up (positive values) indicate enhancement; (b) Fluorescence image of 8-HQ/M^{n+} PC array (λ_{ex}: 430nm).

As shown in Figure 4, various optical signals corresponding to different metal ions can be extracted with automatic microplate reader simultaneously, thus ensuring the same testing environment and greatly saving the time of measurement. For the same concentration of different metal ions, the optical information shows obviously different fluorescence enhancement and quenching effects. On the other hand, varying degree fluorescence amplification and quenching effects come out with corresponding changes of concentration towards the same kinds of metal ions. The fluorescence image of 8-HQ/M^{n+} PCs array was exhibited under the excitation wavelength at 430 nm in Figure 4b. The phenomenon implies that with the employment of CPA chip, single point of fluorescence information acquisition can be converted to *in situ* multiple optical signals extraction.

Quantitative detection of BSA from 96-well plate simultaneous fluorescence response platform.

A considerable amount of techniques about the determination of protein concentration have been well put forth. They mainly include conventional Lowry method, Bradford law and BCA (Bicinchoninic acid) method, among which the BCA method processes the highest sensitivity. The principle of BCA method depends on the complexation of Cu^{2+} with protein in alkaline environment, but some buffer solution may make an impact to the color reactions of the BCA. Notably, the BCA method used for determination of protein of high purity is accurate, so the results may have deviation if the sample was of impure. Universally, there is little fluorescent displaying of fluorescamine (FL), but homologous fluorescent compounds are generated once reacting with amino acid, polypeptide and protein. The maximum excitation wavelength and main emission wavelength of as-reacted compounds are 390 nm and 475 nm respectively. Besides the various compound containing primary amino reported in former literature, we further studied the reaction product of FL and bovine serum albumin (BSA). Appropriate account of FL solution was dropped into the 96-well plate using micropipette (50 μL), which were filled with PC supraballs. After the solvent evaporated, different concentration (10^{-1} - 10^{-8} mM) of BSA solutions (50 μL) were added into the plate in sequence. The fluorescence responses were spotted by automatic microplate reader in five distinct channels (CH1: 470 nm with 390 nm excitation, CH2: 500 nm with 365 nm excitation, CH3: 470 nm with 365 nm excitation, CH4: 500 nm with 430 nm excitation, represented by different colors as blue, green, yellow and red).

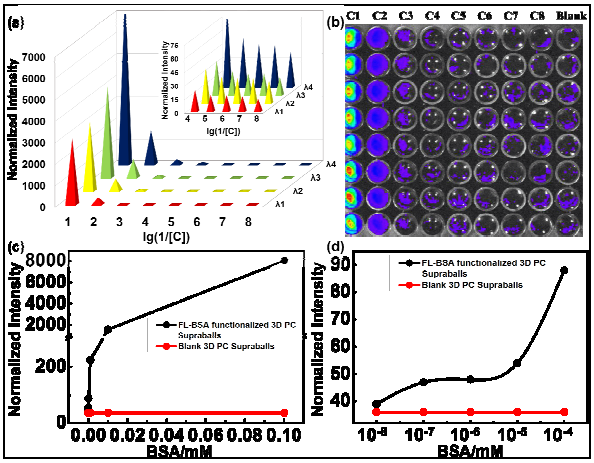

Figure 5. (a) Patterns of different BSA concentrations (10^{-1} - 10^{-8} mM) reacting to FL. The fluorescence change induced in four various excitation and emission channels. Insert: Detail of the concentration (10^{-4} - 10^{-8} mM) region. (b) Fluorescence image of the PC array spotted by 8 different concentrations of BSA solution ($\lambda_{ex:}$ 430 nm); (c) The BSA concentration (10^{-1} - 10^{-8} mM) dependence of the fluorescence intensity reacting to FL based on 3D PC supraballs; (d) Detail of the concentration (10^{-4} - 10^{-8} mM) region.

Figure 5a shows that the fluorescence intensity reduction is as along with the decrease of BSA concentration under the same excitation wavelengths. Moreover, the detection limit here can be reached to 10^{-8} mM equivalently to 10^{-4} mg/L. It also shows the distinction of fluorescence intensity under different excitation wavelengths. The fluorescence image of PCs array spotted by 8 different concentrations of BSA solution was exhibited under the excitation wavelength at 430 nm (Figure 5b). The BSA concentration (10^{-1} - 10^{-8} mM) dependence of the fluorescence intensity reacting to FL based on 3D PC supraballs is shown as Figure 5c-d.Hence, so as to one-off *in situ* detection of protein, such detection method can be developed to obtain a working curve or detection mask.

Conclusions

In summary, we have reported a convenient and robust strategy by setting up the 96-well plate based 3D photonic crystal (PC) supraballs platform, to analyze metal ions and biomolecules *in-situ*. These supraballs were done using monodispersed polystyrene colloids with the addition of 8-hydroxyquinoline, forming 3D PC microdetector towards metal

ions. We also fabricated 2D PC films via vertical deposition method, and found that the effects of different stop-bands on the fluorescence intensity of 8-HQ/Zn^{2+} complex via inkjet printing technology could offer an alternative method for detecting zinc ions. More practice, these supraballs were applied to construct fluorescent probe platform and a cell photonic crystal array (CPA) chip, allowing them to quantitatively test bovine serum albumin (BSA) and 11 kinds of metal ions with 10^{-8} mM level. The selective fluorescence enhancement or quenching effect of CPA chip on different metal ions offers the possibility to identify and analyze multi-analyte. The establishment of the chip provides a more convenient and effective way for extracting and analyzing multi-signals by one-time, having great potential applications in the field of biological detection.

Acknowledgements

This work was supported by National Natural Science Foundation of China (81072682, 21076103, 21474052 and 21176122), Natural Science Foundation of Jiangsu Province (BK20140934), the State Key Laboratory of Pharmaceutical Biotechnology of Nanjing University (02ZZYJ-201302), Priority Academic Program Development of Jiangsu Higher Education Institutions (PAPD), and Qing Lan Project.

References

1 J. M. Weissman, H. B. Sunkara, A. S. Tse and S. A. Asher, *Science,* 1996, **274**, 959-960.
2 E. Centeno and D. Felbacq, *Opt. Commun.*, 1999, **160**, 57-60.
3 Konopsky, N. Valery, Alieva and V. Elena, *Anal. Chem.*, 2007, **79**, 4729-4735.
4 H. Li, J. X. Wang, H. Lin, L. Xu, W. Xu, R. M. Wang, Y. L. Song and D. B. Zhu, *Adv. Mater.*, 2010, **22**, 1237-1241.
5 M. Lopez-Garcia, J. F. Galisteo-Lopez, A. Blanco, J. Sanchez-Marcos, C. Lopez and A. Garcia-Martin, *Small.*, 2010, **6**, 1757-1761.
6 A. Mihi, C. J. Zhang and P. V. Braun, *Angew. Chem. Int. Ed.*, 2011, **123**, 5830-5833.
7 Y. Huang, J. M. Zhou, B. Su, L. Shi, J. X. Wang, S. R. Chen, L. B. Wang, J. Zi, Y. L. Song and L. Jiang, *J. Am. Chem. Soc*., 2012, **134**, 17053-17058.
8 Q. Q. Fu, A. Chen, L. Shi and J. P. Ge, *Chem. Commun.*, 2015, **51**, 7382-7385.
9 J. I. L. Chen, G. Von Freymann, S. Y. Choi, V. Kitaev and G. A. Ozin, *Adv. Mater.*, 2006, **18**, 1915-1919.
10 A. M. Cubillas, M. Schmidt, M. Scharrer, T. G. Euser, B. J. M. Etzold, N. Taccardi, P. Wasserscheid and P. S. Russell, *Chem-Eur. J.*, 2012, **18**, 1586-1590.
11 T. Wang, X. Q. Yan, S. S. Zhao, B. Lin, C. Xue, G. D. Yang, S. J. Ding, B. L. Yang, C. S. Ma, G. Yang and G. R. Yang, *J. Mater. Chem. A.*, 2014, 2, **37**, 15611-15619.
12 X. F. Li, X. Y. Zhang, X. Z. Zheng, Y. Shao, M. He, P. Wang, X. Z. Fu and D. Z. Li, *J. Mater. Chem. A.*, 2014, **2**, 15796-15802.
13 R. Mitchell, R. Brydson and R. E. Douthwaite, *Nanoscale*, 2014, **6**, 4043-4046.
14 F. Sordello and C. Minero, *Appl. Catal. B-Environ.*, 2015, **163**, 452-458.
15 M. Loncar, A. Scherer and Y. M. Qiu, *Appl. Phys. Lett.*, 2003, **82**, 4648-4650.
16 C. E. Reese and S. A. Asher, *Anal. Chem.*, 2003, **75**, 3915-3918.
17 I. B. Burgess, L. Mishchenko, B. D. Hatton, M. Kolle, M. Loncar and J. Aizenberg, *J. Am. Chem. Soc.*, 2011, **133**, 12430-12432.
18 H. Li, J. X. Wang, Z. L. Pan, L. Y. Cui, L. A. Xu, R. M. Wang, Y. L. Song and L. Jiang, *J. Mater. Chem.*, 2011, **21**, 1730-1735.
19 J. T. Zhang, Z. Y. Cai, D. H. Kwak, X. Y. Liu and S. A. Asher, *Anal. Chem.*, 2014, **86**, 9036-9041.
20 J. Hou, H. C. Zhang, Q. Yang, M. Z. Li, Y. L. Song and L. Jiang, *Angew. Chem. Int. Ed.*, 2014, **53**, 5791-5795.
21 X. D. Hong, Y. Peng, J. L. Bai, B. A. Ning, Y. Y. Liu, Z. J. Zhou and Z. X. Gao, *Small*, 2014, **10**, 1308-1313.
22 R. D. Peterson, W. L. Chen, B. T. Cunningham and J. E. Andrade, *Biosens. Bioelectron.*, 2015, **74**, 815-822.
23 F. Frascella, S. Ricciardi, L. Pasquardini, C. Potrich, A. Angelini, A. Chiado, C. Pederzolli, N. De Leo, P. Rivolo and C. F. Pirri, *Analyst.*, 2015, **140**, 5459-5463.
24 A. Ranft, F. Niekiel, I. Pavlichenko, N. Stock and B. V. Lotsch, *Chem. Mater.*, 2015, **27**, 1961-1970.
25 D. Takahashi, S. Hachuda, T. Watanabe, Y. Nishijima and T. Baba, *Appl. Phys. Lett.*, 2015, **106**, 131112.
26 K. Lee and S. A. Asher, *J. Am. Chem. Soc.*, 2000, 122, 9534-9537.
27 Y. J. Lee and P. V. Braun, *Adv. Mater.*, 2003, **15**, 563-566.
28 S. A. Asher, V. L. Alexeev, A. V. Goponenko, A. C. Sharma, I. K. Lednev, C. S. Wilcox and D. N. Finegold, *J. Am. Chem. Soc.*, 2003, **125**, 3322-3329.
29 S. Y. Choi, M. Mamak, G. von Freymann, N. Chopra and G. A. Ozin, *Nano Lett.*, 2006, **6**, 2456-2461.
30 S. Mandal and D. Erickson, *Opt. Express.*, 2006, **16**, 1623-1631.
31 M. Lee and P. M. Fauchet, *Opt. Express.*, 2007, **15**, 4530-4535.
32 X. L. Xu, A. V. Goponenko and S. A. Asher, *J. Am. Chem. Soc.*, 2008, **130**, 3113-3119.
33 J. P. Ge, H. Lee, L. He, J. Kim, Z. D. Lu, H. Kim, J. Goebl, S. Kwon and Y. D. Yin, *J. Am. Chem. Soc.*, 2009, **131**, 15687-15694.
34 H. K. Hunt and A. M. Armani, *Nanoscale*, 2010, **2**, 1544-1559.
35 Y. Q. Zhang, J. X. Wang, Y. L. Shang, Y. L. Song and L. Jiang, *Appl. Phys. A-Mater.*, 2011, **102**, 531-536.
36 H. L. Jiang, Y. H. Zhu, C. Chen, J. H. Shen, H. Bao, L. M. Peng, X. L. Yang and C. Z. Li, *New. J. Chem.*, 2012, **36**, 1051-1056.
37 S. N. Yin, C. F. Wang, S. S. Liu and S. Chen, *J. Mater. Chem. C.*, 2013, **1**, 4685-4690.
38 J. Y. Wang, Y. D. Hu, R. H. Deng, R. J. Liang, W. K. Li, S. Q. Liu and J. T. Zhu, *Langmuir*, 2013, **29**, 8825-8834.
39 B. F. Ye, F. Rong, H. C. Gu, Z. Y. Xie, Y. Cheng, Y. J. Zhao and Z. Z. Gu, *Chem. Commun.*, 2013, **49**, 5331-5333.
40 L. Bai, Z. Y. Xie, W. Wang, C. W. Yuan, Y. J. Zhao, Z. D. Mu, Q. F. Zhong and Z. Z. Gu, *ACS Nano*, 2014, **8**, 11094-11100.
41 S. Aki, T. Endo, K. Sueyoshi and H. Hisamoto, *Anal. Chem.*, 2014, **86** (24), 11986–11991.
42 C. E. Reese and S. A. Asher, *Anal. Chem.*, 2003, **75**, 3915-3918.
43 S. A. Asher, A. C. Sharma, A. V. Goponenko and M. M. Ward, *Anal. Chem.*, 2003, **75**, 1676-1683.
44 L. Y. Cui, W. Shi, J. X. Wang, Y. L. Song, H. M. Ma and L. Jiang, *Anal. Methods*, 2010, **2**, 448-450.
45 M. Z. Li, F. He, Q. Liao, J. Liu, L. Xu, L. Jiang, Y. L. Song, S. Wang and D. B. Zhu, *Angew. Chem. Int. Ed.*, 2008, **47**, 7258-7262.
46 Y. J. Zhao, X. W. Zhao, C. Sun, J. Li, R. Zhu and Z. Z. Gu, *Anal. Chem.*, 2008, **80**, 1598–1605.
47 S. Mandal, J. M. Goddard and D. Erickson, *Lab on Chip*, 2009, **9**, 2924-2932.
48 M. M. W. Muscatello, L. E. Stunja and S. A. Asher, *Anal. Chem.*, 2009, **81**, 4978-4986.
49 W. Z. Shen, M. Z. Li, L. A. Xu, S. T. Wang, L. Jiang, Y. L. Song and D. B. Zhu, *Biosens. Bioelectron.*, 2011, **26**, 2165-2170.
50 S. Pal, P. M. Fauchet and B. L. Miller, *Anal. Chem.*, 2012, **84**, 8900–8908.
51 M. Ben-Moshe, V. L. Alexeev and S. A. Asher, *Anal. Chem.*, 2006, **78**, 5149-5157.
52 H. L. Li, L. X. Chang, J. X. Wang, L. M. Yang and Y. L. Song, *J. Mater. Chem.*, 2008, **18**, 5098-5103.
53 L. D. Bonifacio, G. A. Ozin and A. C. Arsenault, *Small*, 2011, **7**, 3153-3157.
54 G. Z. Deng, K. Xu, Y. Sun, Y. Chen, T. S. Zheng and J. L. Li, *Anal. Chem.*, 2013, **85**, 2833–2840.
55 T. A. Dickinson, J. White, J. S. Kauer and D. R. Walt, *Nature*, 1996, **382**, 697-700.

56 P. C. Jurs, G. A. Bakken and H. E. McClelland, *Chem. Rev.*, 2000, **100**, 2649-2678.
57 K. J. Albert, N. S. Lewis, C. L. Schauer, G. A. Sotzing, S. E. Stitzel, Vaid, T. P.; Walt, D. R. *Chem. Rev.*, 2000, **100**, 2595-2626.
58 A. N. Shipway, E. Katz and I. Willner, *Chemphyschem*, 2000, **1**, 18-52.
59 G. F. Zheng, F. Patolsky, Y. Cui, W. U. Wang and C. M. Lieber, *Nat. Biotechnol.*, 2005, **23**, 1294-1301.
60 A. Star, V. Joshi, S. Skarupo, D. Thomas and J. C. P. Gabriel, *J. Phys. Chem. B.*, 2006, **110**, 21014-21020.
61 M. C. McAlpine, H. Ahmad, D. W. Wang and J. R. Heath, *Nat. Mater.*, 2007, **6**, 379-384.
62 P. Anzenbacher, F. Y. Li and M. A. Palacios, *Angew. Chem. Int. Ed.*, 2012, **51**, 2345-2348.
63 A. Abdelhalim, M. Winkler, F. Loghin, C. Zeiser, P. Lugli and A. AbdellahInstitute, *Sensor. Actuat. B-Chem.*, 2015, **220**, 1288-1296.
64 M. Y. Jia, Q. S. Wu, Li, H. Y. Zhang, Y. F. Guan and L. Feng, *Biosens*. Bioelectron., 2015, **74**, 1029-1037.
65 C. S. Huang, S. George, M. Lu, V. Chaudhery, R. M. Tan, R. C.Zangar and B. T. Cunningham, *Anal. Chem.*, 2011, **83**, 1425–1430.
66 C. S. Huang, V. Chaudhery, A. Pokhriyal, S. George, J. Polans, M. Lu, R. M. Tan, R. C. Zangar and B. T. Cunningham, *Anal. Chem.*, 2012, **84**, 1126–1133.
67 Y. Huang, F. Y. Li, M. Qin, L. Jiang and Y. L. Song, *Angew. Chem. Int. Ed.*, 2013, **52**, 7296-7299.
68 D. Xu, W. Zhu, C. Wang, T. Tian, J. C. Cui, J. Li, H. Wang and G. T. Li, *Chem-Eur. J.*, 2014, **20**, 16620-16625.
69 L. Bai, Z. Y. Xie, K. D. Cao, Y. J. Zhao, H. Xu, C. Zhu, Z. D. Mu, Q. F. Zhong and Z. Z. Gu, *Nanoscale*, 2014, **6**, 5680-5685.
70 S. H. Fan, P. R. Villeneuve, J. D. Joannopoulos and E. F. Schubert, Phys. *Rev. Lett.*, 1997, **78**, 3294-3297.
71 M. Zelsmann, E. Picard, T. Charvolin, E. Hadji, M. Heitzmann, B. Dal'zotto, M. E. Nier, C. Seassal, P. Rojo-Romeo and X. Letartre, *Appl. Phys. Lett.*, 2003, **83**, 2542-2544.

Fabrication of 2D and 3D photonic crystal arrays towards metal ions or biomolecule high performance recognition

Ting Chen[2], Zheng-Yan Deng[2], Su-Na Yin[2], Su Chen[2]* and Chen Xu[1]*

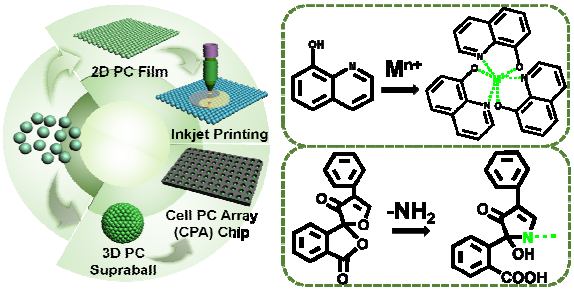

2D and 3D photonic crystal were prepared to detect metal ions via inkjet printing response and single loaded coordination response.

KEYWORDS: photonic crystal; 96-well plate; metal ion detection; biomolecule detection;